Simulation of seismic wave propagation in a poroelastic media: an application to a CO_2 sequestration case

*Emmanuel Anthony[1,2,3], Nimisha Vedanti[1,3]**
1.CSIR-National Geophysical Research Institute, Hyderabad, 500007, India
2. Department of Physics, Imo State University Owerri, Nigeria
3. AcSIR-NGRI, Hyderabad, 500007, India

*email: nimisha@ngri.res.in

Keywords

Poroelasticity, CO_2 injection, Staggered grid, Finite difference, Seismic modelling

Summary

Wave propagation through a porous media allows us to understand the response and interaction that occur between the elastic rock matrix and the fluid. This interaction has been described by Biot in the theory of poroelasticity. We developed a velocity stress staggered-grid finite difference algorithm for the propagation of seismic wave in a poroelatic media using the Biot's formulation. The Biot's equations were discretized using the second order and fourth order approximation for the temporal and spatial grid, respectively. To test our algorithm, we considered two models with the poroelastic properties estimated from well log obtained from Utsira formation, Sleipner, North Sea. The first model represents a homogeneous media with a single layer sandstone saturated with brine; however, the second model is considered as a two-layered homogeneous model, to see the effect of CO_2 injection into the brine formation. As predicted by Biot's theory, the fast and slow compressional waves were observed in the particle velocity snapshots at frequencies higher than the Biot's frequency.

Introduction

The study of seismic wave imaging and inversion of the subsurface properties of the earth are usually carried out with the assumption that the propagating media are acoustic or elastic, which assumed a single-phase theory (Sheen et al., 2006). Seismic methods based on the single-phase acoustic or elastic medium have been successfully used to identify geological structures (Sheen et al., 2006). These approximations are valid in these models, but the properties of the pore fluid such as the density, bulk modulus, viscosity etc. are not considered. Thus, to describe wave propagation in fluid-saturated media, Maurice Biot proposed the theory of poroelasticity (Biot, 1956, 1962).

This theory incorporated or considered the properties of the fluid, which were not accounted for by the single-phase media. Biot also predicted the existence of two compressional waves and one rotational wave in a poroelastic media. When a seismic wave propagates through a porous medium, a pressure gradient is created or we can say that a pressure relaxation is achieved. This pressure difference leads to fluid flow as the fluid moves in the pores with respect to the solid. This process is referred as wave-induced fluid flow, and it is accompanied by the dissipation of energy. The wave-induced fluid flow can be used to monitor the time-lapse seismic response of a reservoir, happening due to change in the fluid properties such as the injection of CO_2 into a reservoir (Morency et al., 2011). In literatures, analytical solutions to the Biot's equations using a simple homogeneous poroelastic media exist (Dai et al., 1995), (Boutin and Bonnet, 1986), and (Burridge and Vargas, 1978). However, for a complex model like in the case of CO_2 injection, a numerical methods like finite difference method (FDM) (Zhu and McMechan, 1991; Dai et al., 1995; Wenzlau and Muller, 2009; Itz et al., 2016; O'Brien, 2010), pseudo-spectral methods (Carcione, 1996b,a; Ozdenvar and McMechan, 1997), finite element method (Roberts and Garboczi, 2002) and spectral element (Morency, 2008) have been used. In the present work, we used the FDM to solve the Biot's equations for the poroelastic media and demonstrate the application of the developed algorithm on the models, prepared using the poroelastic properties derived from the well log data obtained from the Utsira sand, Sleipner field, North Sea.

Simulation of seismic wave propagation in a poroelastic media

Theory

Biot (1956a,b, 1962) established the theory of poroelasticity with these assumptions:

1.The fluid phase is continuous
2.The porous medium is statistically isotropic
3.Seismic wavelength is larger than the pore size
4.Deformations on the elastic rock matrix is small

The Biot's poroelastic equations for an isotropic medium are given by

$$\rho\ddot{\boldsymbol{u}} + \rho_f\ddot{\boldsymbol{w}} = (\lambda_c + \mu)\boldsymbol{u} + \mu\nabla^2\boldsymbol{u} + \alpha M\nabla\nabla.\boldsymbol{w} \qquad (1)$$

$$\rho_f\ddot{\boldsymbol{u}} + m\ddot{\boldsymbol{w}} = \alpha M\nabla\nabla.\mathbf{u} + \mathrm{M}\nabla\nabla.\mathbf{w} - b\dot{\boldsymbol{w}} \qquad (2)$$

where **u** is the solid displacement, **w** the displacement
of the fluid relative to the solid.
The stress and pressure are given by

$$\tau_{ij} = 2\mu e_{ij} + \delta_{ij}(\lambda_c e_{kk} + \alpha M w_{k,k}) \qquad (3)$$

$$p = -\alpha M e_{kk} - M w_{k,k} \qquad (4)$$

where e_{ij} is the strain tensor, δ_{ij} is the Kronecker delta.
The Biot's equations above (equation 1,2,3 and 4) can be written in the velocity-stress formation as proposed by Virieux (1984) as

$$\dot{v}_i = \left(m\rho - \rho_f^2\right)^{-1}(m\tau_{ij,j} + \rho_f p_{,i} + \rho_f b w_i) \qquad (5)$$

$$\dot{w}_i = \left(m\rho - \rho_f^2\right)^{-1}(-\rho_f\tau_{ij,j} - \rho p_{,i} - \rho b w_i) \qquad (6)$$

$$\dot{\tau}_{ij} = \mu\left(v_{i,j} + v_{j,i}\right) + (\lambda_c v_{k,k} + \alpha M w_{k,k})\delta_{ij} \qquad (7)$$

$$p = -\alpha M v_{i,i} - M w_{i,i} \qquad (8)$$

for a homogenous media, the Biot's characteristic frequency is given as

$$\omega_B = \frac{b\phi}{\upsilon\rho_f}$$

where $b = \frac{\eta}{\kappa}$
The physical parameters in the equations above are listed in Table 1

Table 1: Table of constants

Name	Symbol	unit	
Density of mineral	ρ_s	Kg/m^3	
Density of the fluid	ρ_f	Kg/m^3	
Density	ρ	Kg/m^3	$\phi\rho_s + (1-\phi)\rho_f$
Effective fluid density	m	Kg/m^3	$T\rho_f/\phi$
Porosity	ϕ		
Fluid viscosity	η	Pas	
Permeability of the medium	κ	m^2	
Tortuosity	T		
Mobility of the fluid	b	Pas/m^2	
Lame constant	λ_c	Pa	$\lambda + \alpha^2 M$
Shear modulus	μ	Pa	
Fluid storage coefficient	M	Pa	$K_s(1-\phi-\frac{K_d}{K_s}+\frac{\phi K_s}{K_f})^{-1}$
Effective stress	α	Pa	$1 - K_d/K_s$
Solid bulk modulus	K_s	Pa	
Fluid bulk modulus	K_f	Pa	
Drained bulk modulus	K_d	Pa	$\lambda + 2\backslash 3\ \mu$

Discretization of the Poroelastic equations

The poroelastic wave equations (equation 5,6,7 and 8) were discretized using the staggered grid finite difference method after assigning field variables at different positions on the staggered grid, as shown in Figure 1.

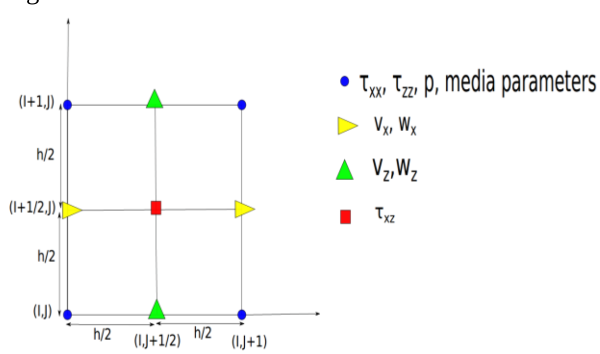

Figure 1: Staggered grid finite difference method for Poroelastic wave equation

In 2D, the discretized poroelastic equations can be written as:

$$D_t v_x = a^2(m(D_x\tau_{xx} + D_x\tau_{xz}) + \rho_f D_x p + \rho_f b\bar{w}_x)$$
$$D_t v_z = a^2(m(D_x\tau_{xz} + D_z\tau_{zz}) + \rho_f D_z p + \rho_f b\bar{w}_z)$$
$$D_t w_x = a^2(-\rho_f(D_x\tau_{xx} + D_x\tau_{xz}) - \rho D_x p - \rho b\bar{w}_x$$
$$D_t w_z = a^2(-\rho_f(D_x\tau_{xz} + D_z\tau_{zz}) - \rho D_z p - \rho b\bar{w}_z$$

$$D_t\tau_{xx} = (2\mu+\lambda_c)D_x v_x + \lambda_c D_z v_z + \alpha M(D_x w_x + D_z w_z)$$
$$D_t\tau_{zz} = (2\mu+\lambda_c)D_z v_z + \lambda_c D_x v_x + \alpha M(D_x w_x + D_z w_z)$$
$$D_t\tau_{xz} = \mu(D_x v_z + D_z v_x)$$
$$D_t p = -\alpha M(D_x v_x + D_z v_z) - M(D_x w_x + D_z v_z)$$

(9)

$$a^2 = \frac{1}{(m\rho-\rho_f^2)}$$

$$D_x\phi(i) = \frac{1}{\Delta x}\left\{\frac{9}{8}\left(\phi\left(i+\frac{1}{2}\right)-\phi\left(i-\frac{1}{2}\right)\right)-\frac{1}{24}\left(\phi\left(i+\frac{3}{2}\right)-\phi\left(i-\frac{3}{2}\right)\right)\right\} \quad (10)$$

The temporal derivatives in equations (9) are replaced by the second-order discrete time differential operator and time averaging as

$$D_t\phi^n = \frac{1}{\Delta t}(\phi^{n+\frac{1}{2}} - \phi^{n-\frac{1}{2}}) \quad (11)$$

$$\dot{\phi}^n = \frac{1}{2}(\phi^{n+\frac{1}{2}} - \phi^{n-\frac{1}{2}}) \quad (12)$$

Absorbing boundary condition

The seismic simulation requires absorbing boundary condition (ABC) to truncate artificial reflections in an unbounded medium. The perfectly matched layer (PML) absorbing boundary condition proposed by (Berenger, 1994) is derived by replacing the coordinate variables in the frequency domain with a complex stretched variable, which is define as

$$\tilde{y} = \int_0^{y_i} z_i(y_i)dy_i$$

where $z_i(y_i) = 1 - \frac{b_i}{i\omega}$, b_i is the damping factor, y_i is the direction and ω is the temporal frequency. The damping factor is defined as $b_i = log\left(\frac{1}{R}\right)\left(\frac{3v_p}{2}\right)\left(\frac{i^2}{L^3}\right)$. R is the coefficient of reflection, and L is the thickness of the PML. In this study, PML is used to truncate the computational domain.

Results

The Utsira formation in the Sleipner field, North Sea is 800m below the sea and is a highly permeable and porous sandstone. CO_2 is being injected into this saline formation since 1994. We estimated the poroelastic properties of the formation (Table 2) and calculated the dry bulk modulus using the Gassmann's equation, using a well log obtained from the Sleipner field.

The Gassmann's equation is given by:

$$K_s = K_d + \frac{\left(1-\frac{K_d}{K_{gr}}\right)^2}{\frac{\varphi}{K_f}+\frac{1-\varphi}{K_{gr}}+\frac{K_d}{K_{gr}^2}} \quad (13)$$

where K_s, K_d, K_{gr}, K_f are bulk moduli of saturated rock, dry rock, grains, and fluid, respectively, and ' φ is the porosity.

Table 2: Saline aquifer and CO_2 in Utsira sand

	Saline water	**CO_2**
ρ_s	2650 kg/m^3	2650 kg/m^3
ρ_f	1090 kg/m^3	650 kg/m^3
ρ	2072 kg/m^3	1910 kg/m^3
K_s	36.9GPa	36.9GPa
K_f	2.3GPa	0.0675Gpa
K_d	2.6815Gpa	2.6815Gpa
μ	0.792145760Gpa	0.792145760Gpa
ϕ	0.37	0.37

1. Homogeneous model

We consider a uniform homogeneous model with dimension 2000m x 2000m with saline aquifer properties as given in Table 2 (Figure 2). Ricker wavelet is used as an explosive source with a dominant frequency of 40Hz. The source is located in the middle of the grid that is (x; z) = (500; 500). The grid step and time step are 2m and 0.2ms respectively.

Figure 3 shows the snapshot of the wave propagation within the seismic frequency. In this frequency regime, one can clearly see that the slow p wave does not propagate because it is diffusive. The slow p wave propagates at frequencies higher than the Biot's frequency or when the diffusive parameter b = 0, as can be seen in Figure 4. This is in line with the predictions of Biot's theory.

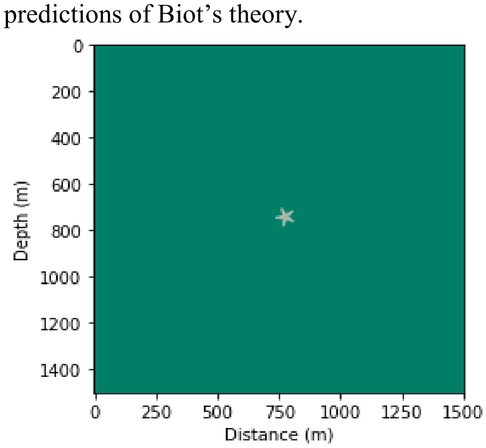

Figure 2: Homogeneous model

Simulation of seismic wave propagation in a poroelastic media

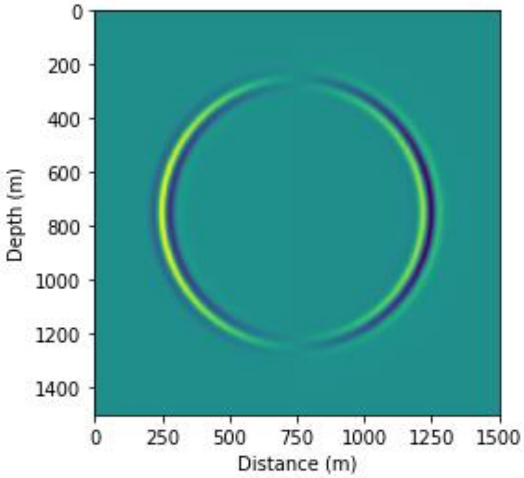

Figure 3: snapshot of vx at a frequency below Biot's frequency

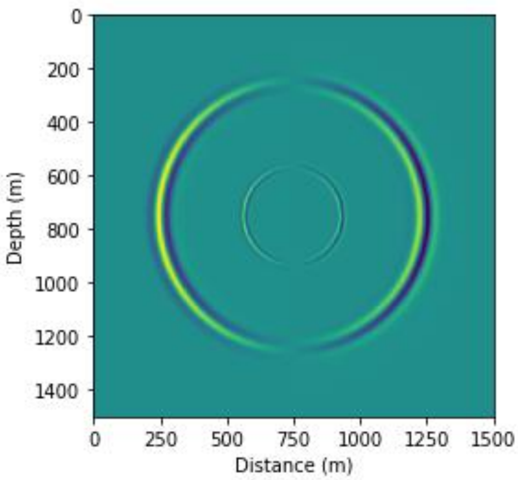

Figure 4: snapshot of vx at a frequency below Biot's frequency

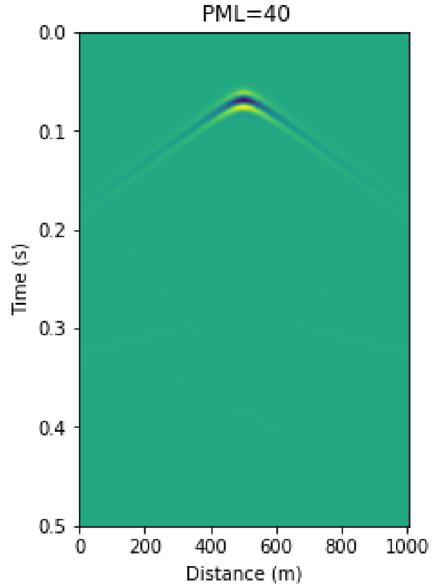

Figure 5: vx shot gather at a frequency below Biot's frequency

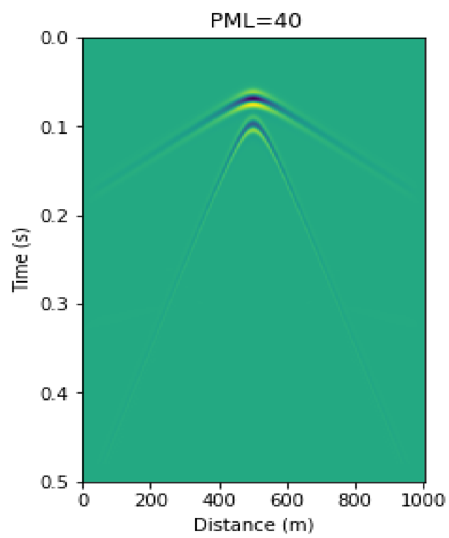

Figure 6: vx shot gather at a frequency above Biot's frequency

2. Two-layer homogeneous model

We designed a model made up of two homogeneous layers (Figure 7). The lower layer contains 100% brine, while the upper layer contains 30% of CO_2 and 70% of brine. The properties of the model is shown in Table 2. Ricker wavelet is used as an explosive source and is located (x; z) = (300; 200). The snapshot and shot gather of the vertical particle velocity are shown in Figure 8, Figure 9, Figure 10 and Figure 11. The slow p wave is generated at a frequency higher than the Biot frequency as expected, and there are some mode conversions at the boundary. These results are in line with the work done by Sheen et al. (2006).

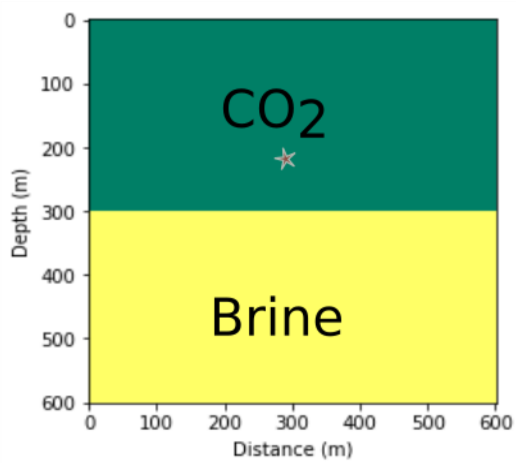

Figure 7: Saline aquifer and CO2 in Utsira sand model

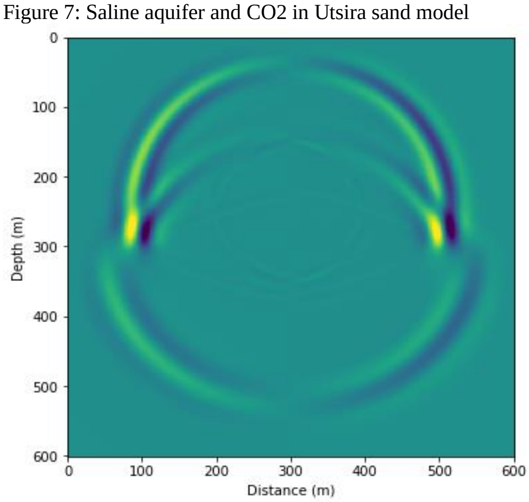

Figure 8: Snapshots of vx at a frequency below Biot's frequency

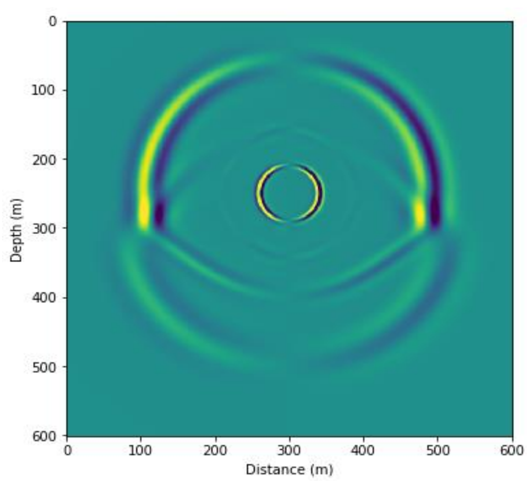

Figure 9: Snapshots of vx at a frequency above Biot's frequency

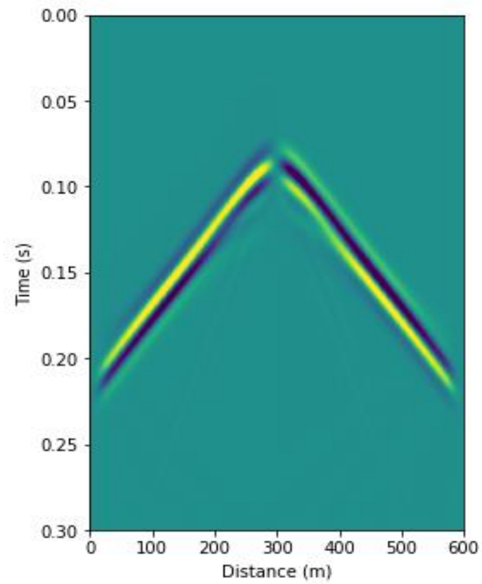

Figure 10: vx shot gather at a frequency below Biot's frequency

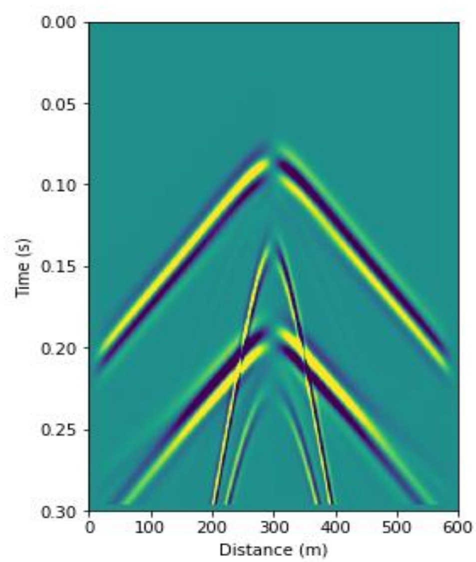

Figure 10: vx shot gather at a frequency above Biot's frequency

Conclusion

In this work, we have developed a velocity stress staggered-grid finite difference algorithm for the propagation of seismic wave in a poroelatic media. We applied the algorithm developed to two types of models with the poroelastic properties estimated from well log data obtained from the Utsira

Simulation of seismic wave propagation in a poroelastic media

Formation, Sleipner, North Sea. As predicted by the Biot's theory, the fast and slow compressional waves were observed in the particle velocity snapshots at frequencies higher than the Biot's frequency.

References

Al-khalifah, T. and Tsvankin, I., 1995, Velocity analysis for transversely isotropic media; Geophysics, 60, 150-1556.

Berenger, J., 1994, A perfectly matched layer for the absorption of electromagnetic waves; Journal of Computational Physics, 114, 185-200.

Biot, M., 1956, Theory of propagation of elastic waves in a fluid saturated porous solid, part i: Low frequency range; J. Acoust. Soc. Am., 28(2), 168-178.

Biot, M., 1956, Theory of propagation of elastic waves in a fluid saturated porous solid, part ii: High frequency range; J. Acoust. Soc. Am., 28(2), 179-191.

Biot, M., 1962, Mechanics of deformation and acoustic propagation in porous media; J. Appl. Phys., 33(4), 1482-1498.

Boutin, C. and Bonnet, P. Y., 1986, Green's functions solutions and associated sources in infinite and stratified poroelastic media; Journal of Geophysical Research, 90, 521-550.

Burridge, R. and Vargas, C. A., 1978, The fundamental solution in dynamic poroelasticity; Journal of Geophysical Research, 58, 61-90.

Carcione, J., 1996, Full frequency-range transient solution for p-wave in a fluid-saturated viscoacoustic porous medium; Geohysical Prospecting, 44, 99-129.

Carcione, J., 1996b, Wave propagation in anisotropic, saturated porous media: Plane-wave theory and numerical simulation; J. acoust. Soc. Am, 99, 2655-2666.

Dai, N., Vafidis, A., and R., K. E., 1995, Wave propagation in heterogeneous, porous media: A velocity-stress, finite-difference method; Geophysics, 60(2), 327-340.

Itz, R., Iturrarn-Viveros, U., and Parra, J. O., 2016, Optimal implicit 2-d finite differences to model wave propagation in poroelastic media; Geophysical Journal International, 206(2), 1111-1125.

Morency, C., Luo, Y., and Tromp, J., 2011, Acoustic, elastic and poroelastic simulations of co2 sequestration monitoring based on spectral-element and adjoint methods; Geophys. J. Int, 185, 955-966.

Morency, C. T. J., 2008, Spectral-element simulations of wave propagation in porous media; Geophys. J. Int, 175, 301-345.

O'Brien, G. S., 2010, 3d rotated and standard staggered finite-difference solutions to biots poroelastic wave equations: Stability condition and dispersion analysis; Geophysics, 75(4), T111-T119.

Ozdenvar, T. and McMechan, G., 1997, Algorithms for staggered-grid computations for poroelastic, elastic, acoustic, and scalar wave equations; Geophys. Prospect, 45,403-420.

Roberts, A. P. and Garboczi, E. J., 2002, Computation of the linear elastic properties of random porous materials with a wide variety of microstructure; Proceedings of the Royal Society of London, 458, 1033-1054.

Sheen, D.-H., Tuncay, K., Baag, C.-E., and Peter, J. O.,,2006, Parallel implementation of a velocitystress staggered-grid finite-difference method for 2-d poroelastic wave propagation; Computers and Geosciences, 32, 1182-1191.

Virieux, J., 1984, Sh-wave propagation in heterogeneous media: velocity-stress finite-difference
method; Geophysics, 49(11), 1933-1942.

Wenzlau, F. and Muller, T. M., 2009, Finite difference modeling of wave propagation and diffusion in poroelastic media; Geophysics, 74(4), T55-T66.

Zhu, X. and McMechan, G., 1991. Finite difference modeling of the seismic response of fluid saturated, porous, elastic solid using biot theory; Geophysics, 56(3), 328-339.

Acknowledgments

Emmanuel Anthony wishes to acknowledge CSIRTWAS for the award of the fellowship. Authors are grateful to the Director NGRI and AcSIR coordinator for their support and permission to publish this work